



Supporting Information

© Wiley-VCH 2007

69451 Weinheim, Germany

Probing Inducible Nitric Oxide Synthase with a Pterin-Ru(II) Sensitizer Wire

Edith C. Glazer, Yen Hoang Le Nguyen, Harry B. Gray and David B. Goodin*

Division of Chemistry and Chemical Engineering, California Institute of Technology, Pasadena, CA 91125, and Department of Molecular Biology, The Scripps Research Institute, 10550 North Torrey Pines Road, La Jolla, CA 92037

Supporting Information

1. Synthesis

Compound **2** was prepared by a procedure modified from Ref. 11. Compound **1** (0.5 g, 2.1 mmol) was suspended in dry DMF (100 mL) and DMF-acetal (3.6 mL, 21 mmol) was added. The solution was stirred at 50 °C for 2 hr., and the crude product diluted with MeOH (1:2) and purified by flash chromatography (silica, MeOH) to give the product (0.56 g, 92% yield).

Compound **3**. Compound **2** (0.2 g, 0.7 mmol) and K₂CO₃ (0.19 g, 1.4 mmol) were suspended in DMF (50 mL) and stirred at room temperature for 0.5 hr. To this solution was added ethyl 6-bromohexanoate (0.6 mL, 3.4 mmol) and the solution was stirred at room temperature for 4 hr. The solvent was removed under reduced pressure, and the product purified by flash chromatography (silica, CH₂Cl₂ ramp to 5% MeOH/CH₂Cl₂) to give the product (0.2 g, 68% yield). ¹H NMR (CDCl₃) δ 9.21 (s, 1H), 9.01 (s, 1H), 8.15 (d, *J*=7.7 Hz, 2H), 7.52–7.45 (m, 3H), 4.37 (t, *J*=7.7 Hz, 2H), 4.12 (q, *J*=6.9 Hz, 2H), 3.65 (s, 3H), 3.28 (s, 3H), 2.31 (t, *J*=7.7 Hz, 3H), 1.84–1.57 (m, 4H), 1.49–1.40 (m, 2H), 1.27–1.23 (m, 2H). ESI-MS calculated for C₂₃H₂₉N₆O₃ [M+H]⁺ 437.5, found 437.4.

Compound **4**. Compound **3** (0.2 g, 0.46 mmol) was dissolved in 1 M NaOH/DMF (40 mL, 1:1) and stirred at room temperature for 1 hr. The solution was neutralized with 1 M HCl, the product extracted into CHCl₃ (5 x 50 mL), dried over MgSO₄ and the solvent removed to give the product (0.13g, 82% yield). ¹H NMR (DMSO-*d*₆) δ 9.31 (s, 1H), 9.05 (br s, 1H), 8.12 (d, *J*= 7.3 Hz, 2H), 8.03 (br s, 2H), 7.54–7.46 (m, 3H), 3.97 (t, *J*=6.1 Hz, 2H), 2.20 (t, *J*=7.3 Hz, 2H), 1.60–1.50 (m, 4H), 1.36–1.34 (m, 2H). ESI-MS calculated for C₁₈H₁₉N₅O₃ [M+H]⁺ 354.4, found 354.3.

Compound **5**. Compound **3** (50 mg, 0.11 mmol) was dissolved in a saturated solution of NH₃/MeOH in a pressure tube, and stirred at room temperature for 18 hr. After the reaction was complete, the solvent was removed to give the product (35 mg, 85 % yield). ¹H NMR (DMSO-*d*₆) δ 9.29 (s, 1H), 8.11 (d, *J*=7.7 Hz, 2H), 7.65 (br s, 2H), 7.54–7.46 (m, 3H), 7.21 (br s, 1H), 6.68 (br s, 1H), 3.97 (t, *J*=7.3 Hz, 2H), 2.30 (t, *J*=7.3 Hz, 2H), 1.60–1.54 (m, 4H), 1.35–1.31 (m, 2H). ESI-MS calculated for C₁₈H₂₁N₆O₂ [M+H]⁺ 353.4, found 353.5.

Compound **6**. Compound **4** (80 mg, 0.23 mmol), EDCI (65 mg, 0.34 mmol) DMAP (42 mg, 0.34 mmol) and (4-hydroxymethyl-4'-methylbpy)Ru(bpy)₂•2PF₆ (300 mg, 0.34 mmol) were dissolved in dry pyridine (20 mL) under argon, and stirred at room temperature for 24 hr. The solvent was removed under reduced pressure and the product purified by flash chromatography (silica, 0.1% KNO₃ (saturated solution)/5% H₂O/MeCN ramp to 1% KNO₃/10% H₂O/MeCN) to give the product (170 mg, 68% yield). The Ru(II) complex was isolated after column purification by solvent removal, dissolving the crude into H₂O, addition of a saturated aqueous solution of KPF₆, and extraction of the complex into CH₂Cl₂. ¹H NMR (MeCN-*d*₃) δ 9.08 (s, 1H), 8.51–8.41 (m, 5H), 8.08–7.97 (m, 6H), 7.80–7.73 (m, 5H), 7.55 (d, *J*=5.88 Hz, 2H), 7.45–7.35 (m, 7H), 7.24 (d, *J*=5.88 Hz, 2H), 6.65 (s, 2H), 4.00 (t, *J*=7.7 Hz, 2H), 2.52 (s, 2H), 2.48 (t, *J*=7.33 Hz, 2H), 2.35 (s, 3H), 1.76–1.66 (m, 4H), 1.84–1.42 (m, 2H). ESI-MS calculated for C₅₀H₄₅F₆N₁₁PRu [M]⁺ 1094, found 1094 [M]⁺, 475 (M²⁺ -PF₆). The counter ions of the Ru(II) complex were converted to the chloride by precipitation from acetone with Bu₄NCl.

2. Methods and data analysis

NMR spectra were obtained on a Varian Mercury 400 MHz spectrometer, and chemical shifts are reported relative to the residual solvent signal. All chemicals were obtained from commercial sources and were used without further purification. All steady state absorption and emission studies were performed in 40 mM EPPS, 1 mM DTT, 10% glycerol, pH 7.6. All time resolved experiments were done in buffer containing 50 mM KPi, 5 mM DTT and 100 mM KCl. Absorption spectra were collected using an HP8453 diode array spectrophotometer. Steady state emission spectra were obtained on a Perkin Elmer LS 50B luminescence spectrometer. Time-resolved fluorescence experiments were performed on air-equilibrated samples as described previously.^{3a,d} Luminescence decays were fit using Origin 7.0, and the distance between donor and acceptor was determined using Förster energy transfer parameters as described previously.^{3d} A value of 1.4 was used for the refractive index, n , and R_0 was calculated to be 22 Å for this system. Luminescence decay kinetics for the free wire were well fit to a single exponential, while two exponentials were required to fit the decay in the presence of iNOS_{heme}.

3. Complete reference 8a

Kotsonis, P.; Frohlich, L. G.; Raman, C. S.; Li, H.; Berg, M.; Gerwig, R.; Groehn, V.; Kang, Y.; Al-Masoudi, N.; Taghavi-Moghadam, S.; Mohr, D.; Munch, U.; Schnabel, J.; Martasek, P.; Masters, B. S. S.; Strobel, H.; Poulos, T.; Matter, H.; Pfeleiderer, W.; Schmidt, H. H. H. W. *J. Biol. Chem.* **2001**, *276*, 49133–49141.

4. Supplemental Figures

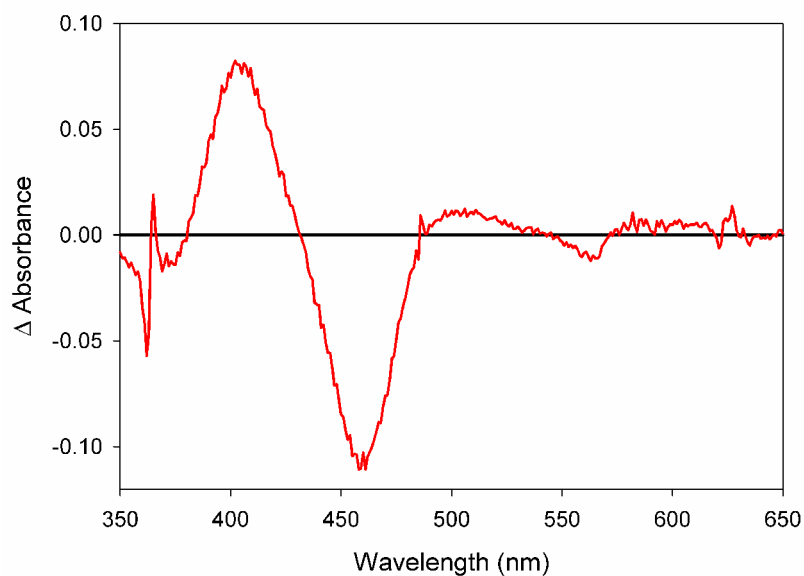


Figure S1. Difference spectra obtained by subtracting the initial, DTT-equilibrated spectra from that recorded after incubating with wire **6** ($50 \mu\text{M}$) for 2 hours.

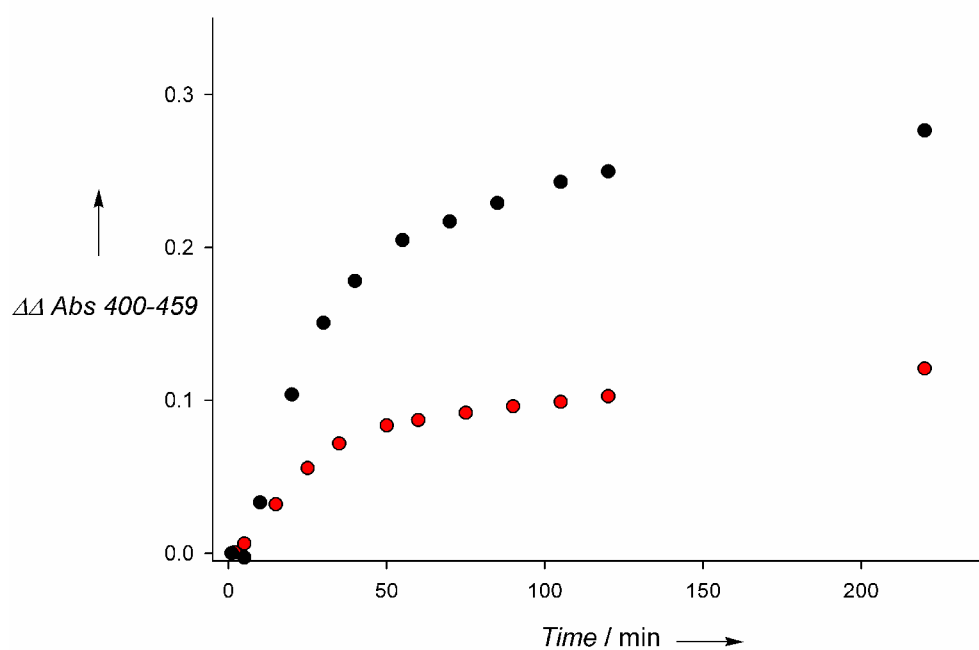


Figure S2. Time dependence of the spectral shift obtained upon reconstitution of $\text{iNOS}_{\text{heme}}$ with wire **6** (red circles; derived from the experiments in Figure 1) compared to H₄B (black circles; $50 \mu\text{M}$ H₄B).

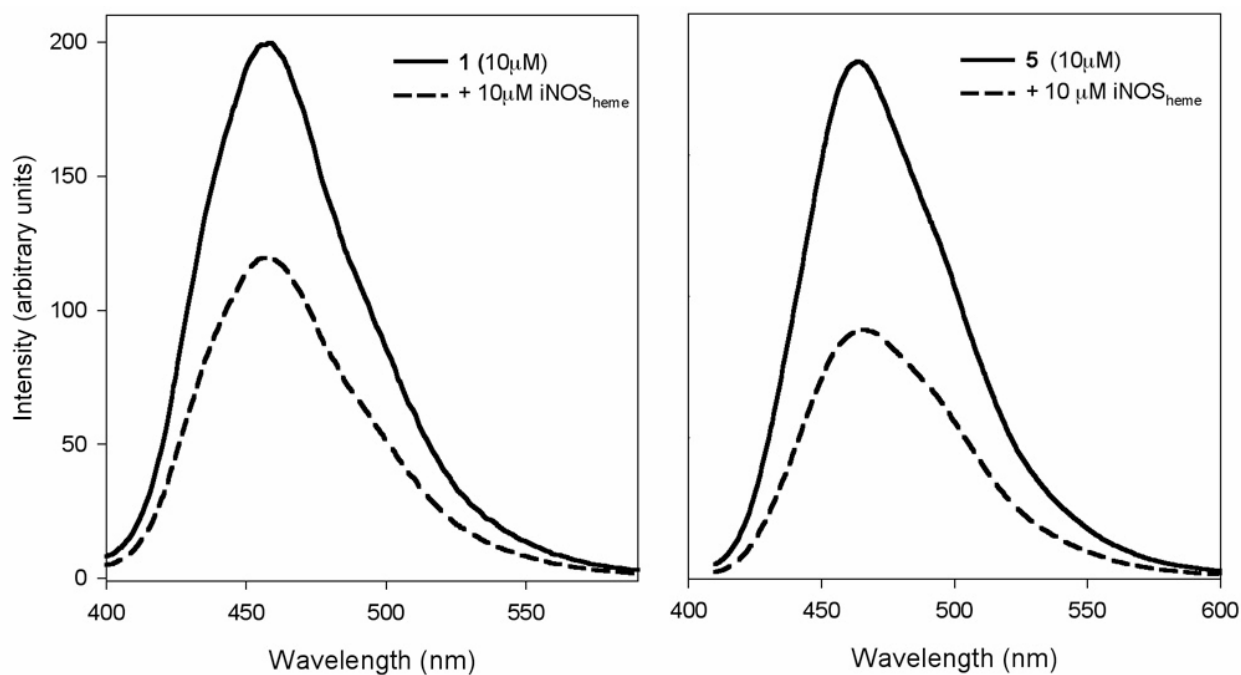


Figure S3. Steady state emission spectra of pterin **1** (left panel, 10 μM , solid line) and **5** (right panel, 10 μM , solid line), and each pterin in the presence of 10 μM iNOS_{heme} (dashed line), showing quenching of emission by the enzyme. The samples were incubated for 2 hr at 0° C before measurement. Emission was stimulated by excitation at 380 nm.

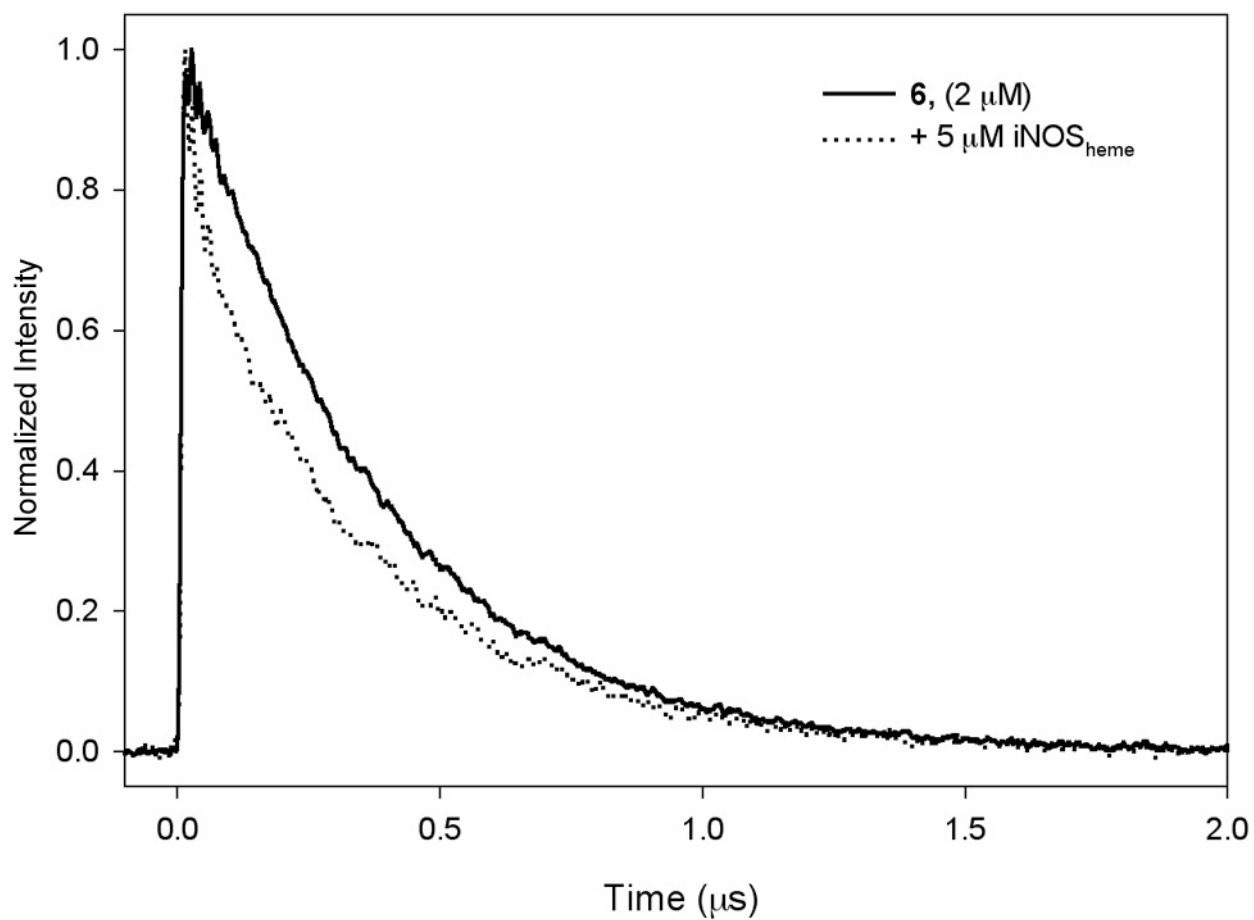


Figure S4. Time resolved emission decay of 2 μM samples of **6** before (solid line) and after addition of 5 μM iNOS_{heme} (dotted line). Excitation was performed at 470 nm and detection at 630 nm. Addition of iNOS_{heme} induces quenching of the Ru(II) emission, evidenced by introduction of a fast decay component.

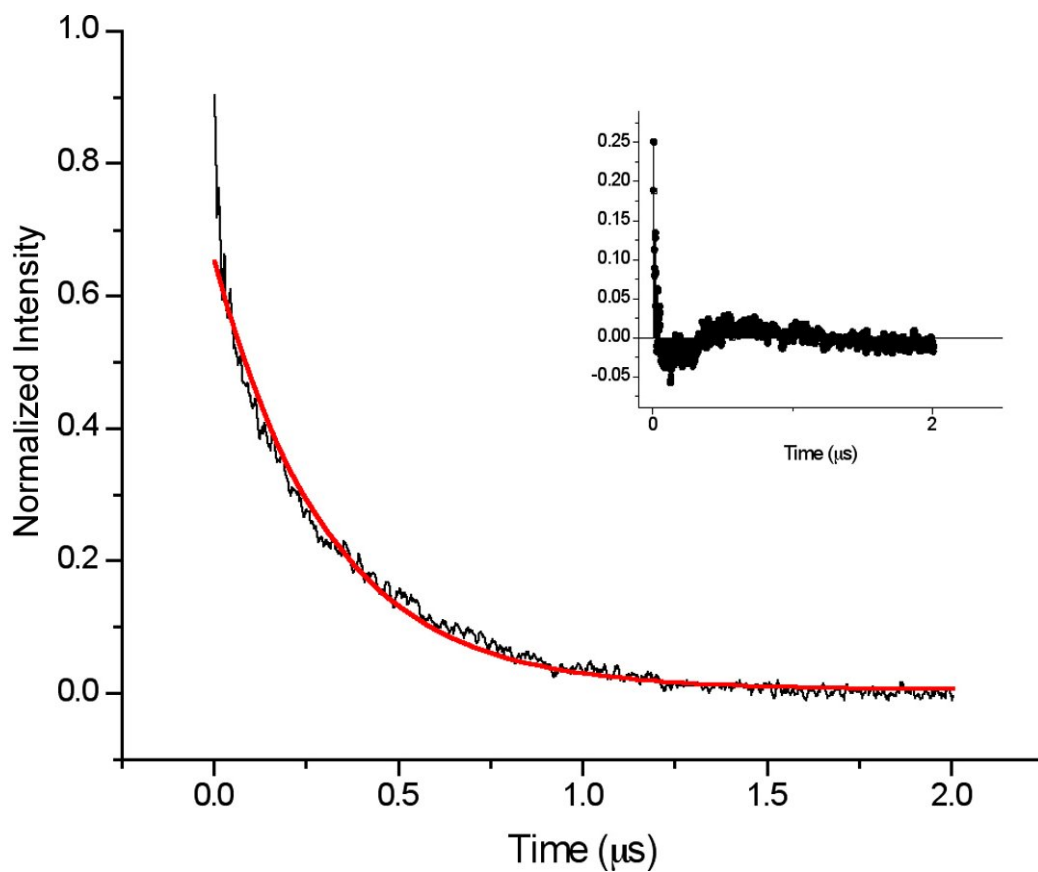


Figure S5. Time resolved emission decay of 2 μM **6** in the presence of 5 μM $\text{iNOS}_{\text{heme}}$ (black) superimposed on the least squares fit to a single exponential with $\tau=305$ ns (red). Fit residual is shown in the inset. Excitation was performed at 470 nm and detection at 630 nm.

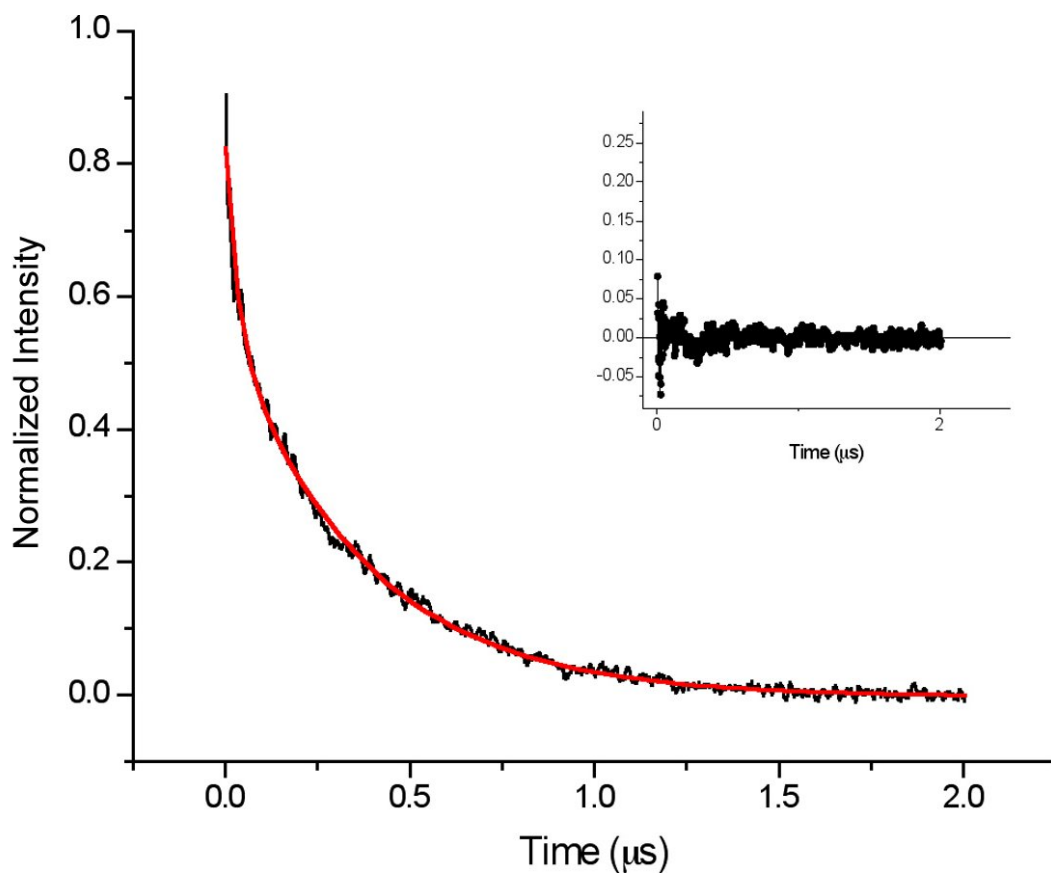


Figure S6. Time resolved emission decay of the data from Figure S4 (black) superimposed on the least squares fit to a biexponential with $\tau_1=376$ ns, and $\tau_2=38$ ns and respective amplitudes of 0.55 and 0.25 (red). Residuals are shown in the inset. Excitation was performed at 470 nm and detection at 630 nm.

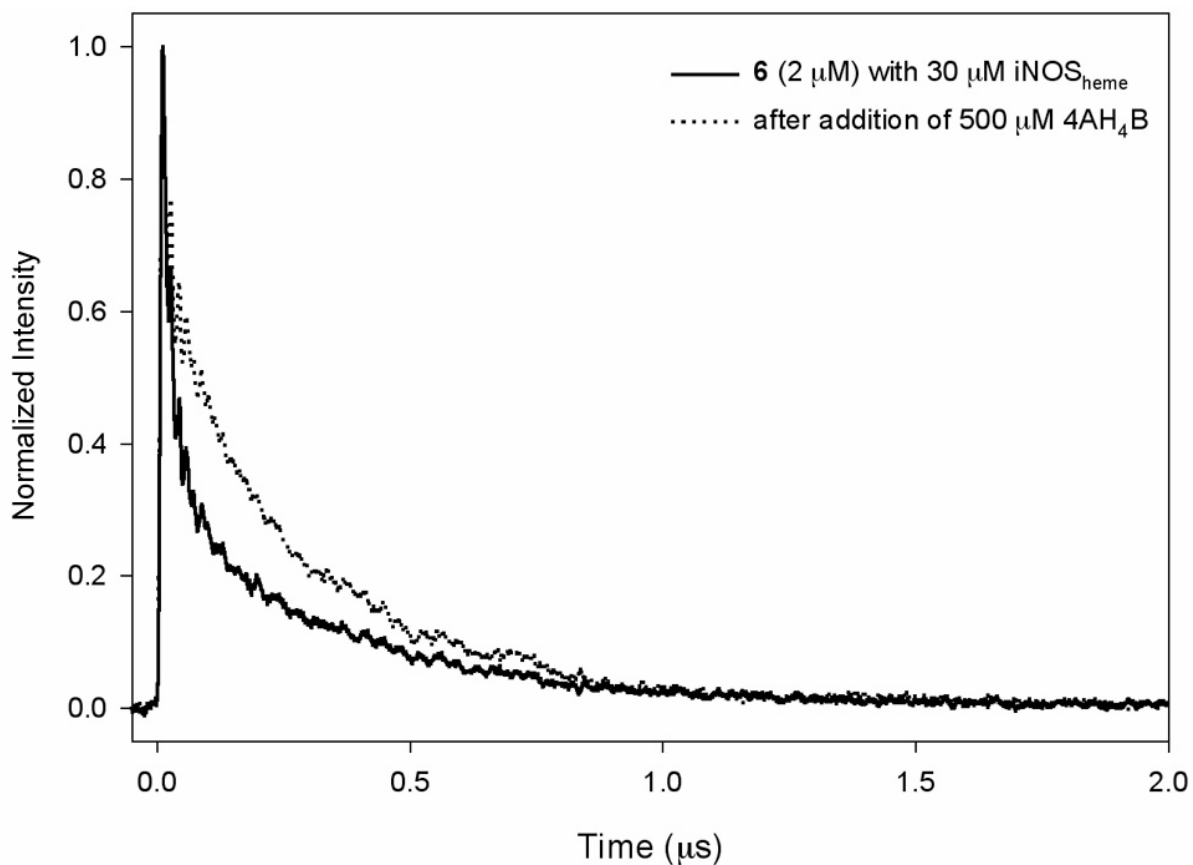


Figure S7. Luminescence decay of 2 μM **6** after incubation in the presence of 30 μM iNOS_{heme} (solid line) and the same solution after the addition of 500 μM 4AH₄B (dotted line). Excess 4AH₄B was used to induce complete displacement of the wire from the protein. The recovery of the monoexponential emission decay indicates displacement of the wire from the protein.

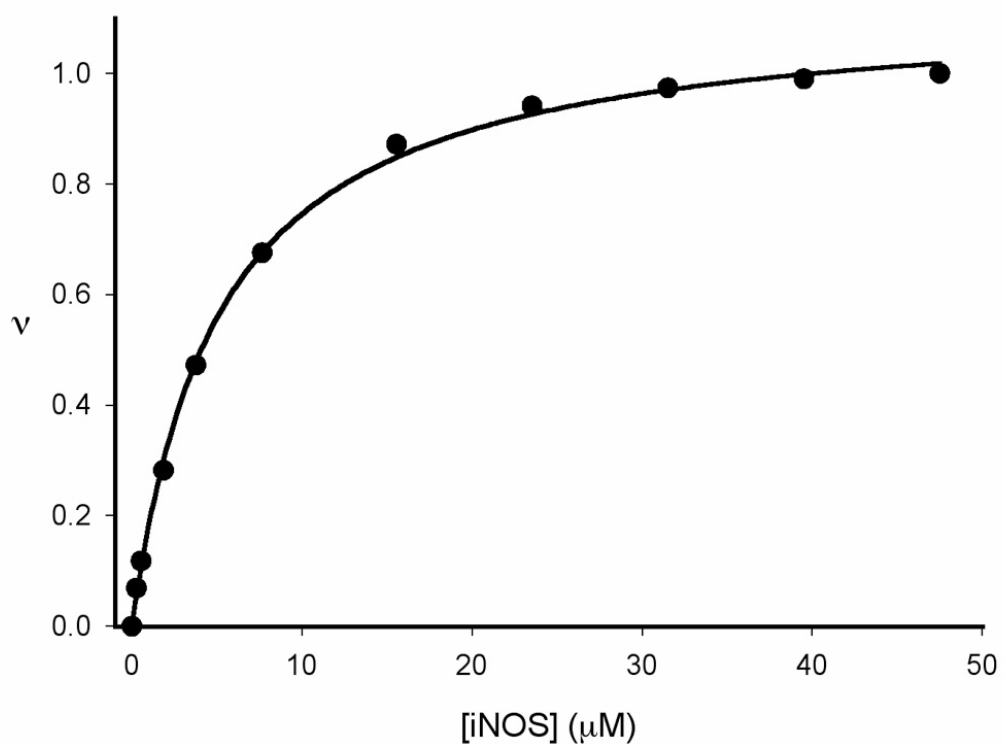


Figure S8. Binding of compound **5** to $iNOS_{\text{heme}}$ measured by steady state fluorescence quenching. The fractional change in total fluorescence intensity (380 nm excitation, 470 nm emission) was measured for samples containing $0.5 \mu\text{M}$ **5** after 20 min equilibration at 0°C following each sequential addition of $iNOS_{\text{heme}}$. Values of $[iNOS_{\text{heme}}]_{\text{total}}$ were corrected for dilution and $[iNOS_{\text{heme}}]_{\text{free}}$ determined from the fraction bound by assuming a 1:1 complex. Data were fit to a single-site model with $K_d=5.1\pm 1 \mu\text{M}$.

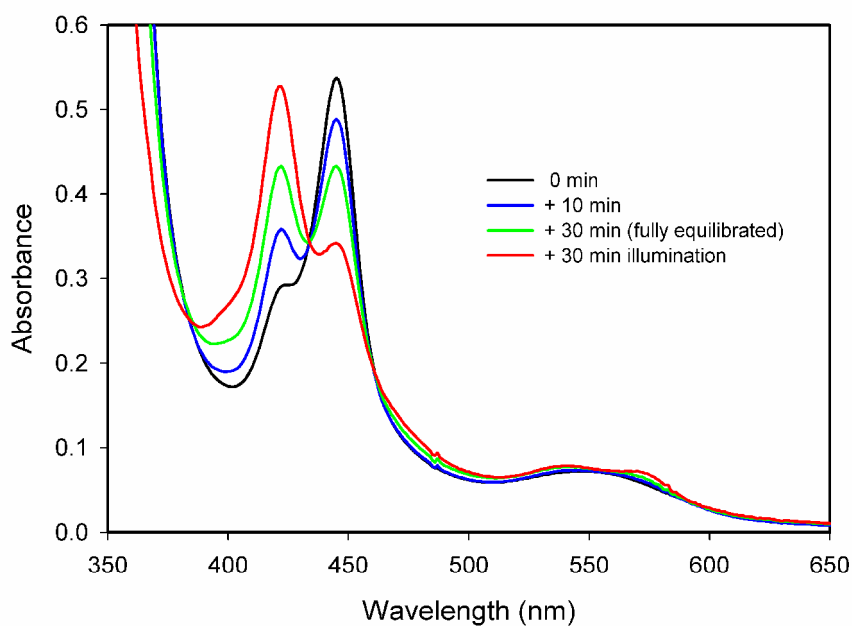


Figure S9. Control experiment showing photolysis of the CO-bound heme to form the P-420 form. Chemical reduction of a sample of $i\text{NOS}_{\text{heme}}$ with H_4B under an atmosphere of CO results in formation of primarily the P-450 species (black line), which evolves over time to form a mixture of the P-450 and P-420 species (blue line, 10 min, green line, 30 min). Subsequent photoexcitation causes further conversion to the P-420 form (red line, 30 min illumination).

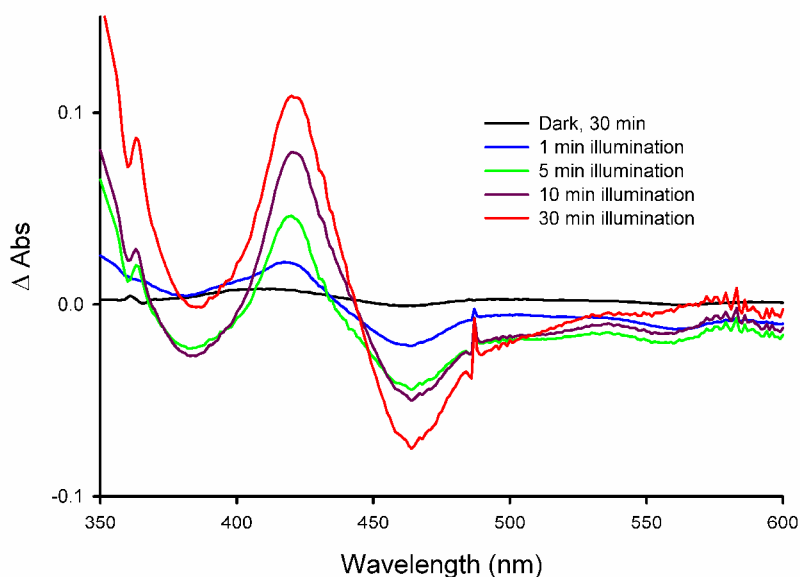


Figure S10. Time dependence of photoreduction of $i\text{NOS}_{\text{heme}}$ ($10 \mu\text{M}$) with wire **6** ($50 \mu\text{M}$) in the presence of 1 mM TMPD in a CO saturated buffer solution at $25 \text{ }^\circ\text{C}$. Increasing illumination time (using 450 nm light) causes an increase in the difference spectra. Incubation of the wire:enzyme complex under identical conditions, but in the dark, produced no change in the difference spectra (black line).

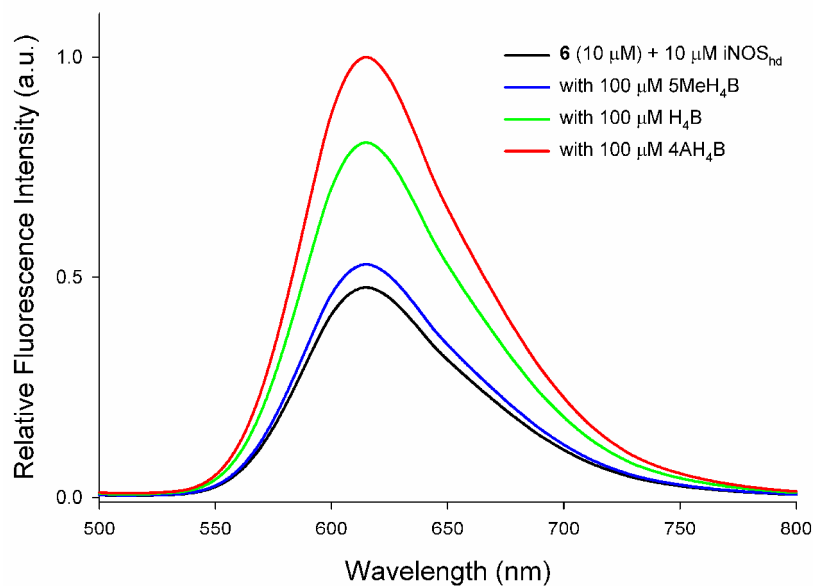


Figure S11. Fluorescence screening of pterin-site binders. The ability of various pterins to displace wire **6** from iNOS_{heme} was tested by measuring the increase in emission of the wire. 5MeH₄B (a very weak binder, blue line) caused only a slight increase in the fluorescence intensity, compared to the native cofactor (H₄B, green line) and the potent inhibitor 4AH₄B (red line). Excitation was performed at 450 nm.